International Journal of Electrical, Electronic and Communication Sciences
ISSN: 2517-9438
Vol:9, No:10, 2015

Model Predictive Control of Three Phase Inverter for PV Systems

Irtaza M. Syed, Kaamran Raahemifar

***Abstract*—**This paper presents a model predictive control (MPC) of a utility interactive three phase inverter (TPI) for a photovoltaic (PV) system at commercial level. The proposed model uses phase locked loop (PLL) to synchronize the TPI with the power electric grid (PEG) and performs MPC control in a dq reference frame. TPI model consists of a boost converter (BC), maximum power point tracking (MPPT) control, and a three-leg voltage source inverter (VSI). The operational model of VSI is used to synthesize the sinusoidal current and track the reference. The model is validated using a 35.7 kW PV system in Matlab/Simulink. Implementation results show simplicity and accuracy, as well as reliability of the model.

***Keywords*—**Model predictive control, three phase voltage source inverter, PV system, Matlab/Simulink.

I. Introduction

GROWING interest in integration of renewable energy systems at various levels of power electric grids (PEG) [1]-[3] has drawn researchers' interest to exploring different VSI control techniques. Photovoltaic (PV) and wind have seen tremendous growth worldwide [4], [5]. VSI at the heart of PV systems, is used to convert PV array produced DC power into AC power suitable for PEG and/or load [6]. The DC power source at the input is not limited to PV though, rectifiers, batteries, and fuel cells can also be used.

In general, VSI consists of a DC-DC converter (Boost Converter, BC), maximum power point tracking (MPPT) control and a DC to AC converter as a single unit. Sine or space vector pulse width modulation (SPWM and SVPWM) with a phase locked loop (PLL) and MPPT are the usual choice of control. Semiconductor switches are used to control and adjust the output parameters [7]. Anti-parallel diodes are connected across the switches to add a reverse current capability [8].

Broadly, VSIs are either classified as current source and voltage source inverters or utility interactive and stand-alone inverters. Alternatively, VSIs are identified as micro, string and central inverters based on their kW ratings. Micro-inverters on module level have less than or equal to 300W power [9], [10]. Single phase inverters (usually few kW) with a control in synchronous reference frame have been discussed in [11], and those with model predictive control (MPC) have been reported by [12]. Three phase VSIs (usually 5 kW to 100s of kW) have been reported with pulse width modulation (PWM) control [13], space vector PWM (SVPWM) [14], and MPC [15]. In [16] we reported comparative analysis of SVPWM and MPC controls for VSI. Repetitive [17], dead-beat [18], and discrete-time sliding-mode [19] controls have also been examined before. MPC of single phase inverters have been reported in [20] and three phase VSI in [21].

Repetitive control [17] has excellent ability to eliminate periodic disturbances; however, it suffers from poor tracking accuracy and poor non-periodic disturbance rejection ability. Complexity and sensitivity to parameter variations and loading conditions are the main problems with deadbeat [18], and Synchronous Reference Frame [12] controls. These controls use conventional PI regulators that require adjustments, two orthogonal signals, and have poor disturbance rejection capability due to the limited gain regulators. MPC for utility interactive seven-level single phase inverter for system application is reported in [20] and focuses on total harmonic distortion (THD and phase reduction through multiple levels. MPC for three phase four-leg inverters is reported by [15] and neutral point clamped three phase VSI for wind systems is reported by [22].

In feedback controllers correction takes place after the error has occurred. However, in MPC the predictive control allows fixing errors before they occur. In the past, MPC has been used for industrial control. Recently, due to its ease of implementation, constraints inclusion, inherent feedback and predictive control, MPC has been applied for controlling power converters. MPC considers a model of the system in order to predict its future behavior. Appropriate switching state is selected based on the present operational status and an objective function that represents the desired behavior of the system in the next interval (future).

This paper presents a simple and easy-to-implement approach of modeling MPC based on TPI for PEG tied PV systems. The rest of the paper is organized into the following sections: (II) PV System, (III) TPI, (VI) MPC, (V) Simulation Results, and (VI) Conclusion.

II. PV System

Fig. 1 shows a typical PV system with central inverter. A PV system consists of a number of PV modules connected in series or parallel to create a DC PV array. The PV array is distributed among several subarrays connected to combiner boxes. The combiner boxes are connected to a common re-combiner box to minimize the number of cables. These combiner boxes are usually arc fault current interrupter (AFCI) with disconnects integrated within them. Otherwise, separate AFCI and disconnects are required. The output of re-

Irtaza M. Syed (student) and Dr. Kaamran Raahemifar (Associate Professor) are with the Electrical & Computer Engineering Department, Ryerson University, Toronto, ON M5K 2K3 Canada (phone: 647-787-6262; e-mail: i5syed@ ryerson.ca, kraahemi@ee.ryerson.ca).

combiner box is connected to a VSI for DC to AC conversion. VSI converts DC into AC at PEG frequency; however, the output voltage of VSI may differ from PEG voltage. A transformer is connected at the output of inverter (sometimes the transformer is integrated in the VSI enclosure) to provide isolation and/or voltage step-up to match the PEG voltage. Finally, the transformer is connected through a metering cabinet and fused AC disconnect to the PEG. All DC and AC cables, fuses and circuit breakers are sized according to the code.

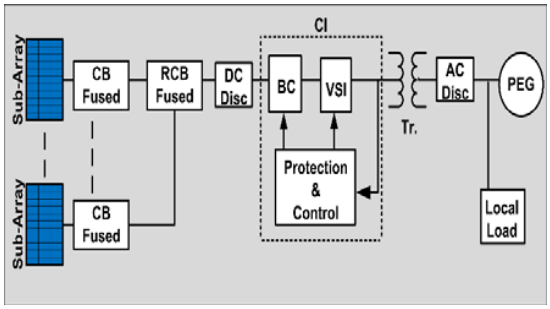

Fig. 1 PV System

Sunlight is converted into DC power by PV modules and the power is supplied across BC for power optimization. Optimally controlled voltage is applied across VSI that generates output AC power from input DC power. The output power is supplied to a local load and/or exported into PEG. The exported power can be stored in PEG and retrieved later to be consumed locally or by other customers connected to the PEG. VSI continuously observes the PEG voltage and frequency levels and disconnects in case of any abnormality to cease exporting power to PEG.

III. Three Phase Inverter

A TPI for PEG tied PV systems consists of a DC-DC converter (usually BC) connected to a PV array with MPPT control for optimal operation, PLL for PEG synchronization, and VSI for DC to AC conversion with some sort of control scheme.

A. Boost Converter

PV array output parameters vary with changes in irradiance and/or temperature. PV current is directly proportional to irradiance (light) and PV voltage is inversely proportional to temperature. Therefore, BC is used to ensure the required fixed voltage of equal to or greater than $\sqrt{2}$Vsys, given by (1), for all irradiance and temperature conditions. The output voltage of BC is calculated by (2), with duty cycle, D, obtained by (3). Capacitor C for BC is sized according to the accepted amount of output voltage ripple using (4) and BC is operated in CCM mode by $L > L_{min}$ (5).

$$V_{DC} \geq \sqrt{2}V_{sys} \quad (1)$$

$$V_O = \frac{1}{1-D}V_{DC} \quad (2)$$

$$D = \frac{t_{on}}{T} \quad (3)$$

$$C_O = \frac{I_O}{\Delta V_O}DT \quad (4)$$

$$L \geq L_{min} = \frac{T}{2I_{LB}}D(1-D)V_O \quad (5)$$

B. MPPT Control

The maximum power point (P_{mp}), a point of operation for a PV array with maximum voltage (V_{mp}) and maximum current (I_{mp}), is ensured using perturb and observe (PO) MPPT algorithm (Fig. 2). To ensure $P_{mp,}$ this iterative control algorithm continuously adjusts PV array voltage and current based on the prevailing irradiation and temperature [10].

C. Phase Locked Loop

In an AC power system, synchronization is the process of matching the frequency of a VSI with that of the PEG for power export into the grid. Phase-Locked Loop (PLL), a closed loop frequency control system, is used to synchronize TPI with the PEG. Park's/Clark's transformations are usually used to convert PEG AC quantities into *dq* DC quantities for synchronization as well as control. V_d, the direct component of voltage, is terminated (not used) and V_q, quadrature component of voltage, is regulated to zero by a PI controller. Angular velocity, ω, is integrated to obtain theta, θ. Theta is reset every cycle (2π) by Mod(2π) to start a new cycle in synchronism with the PEG.

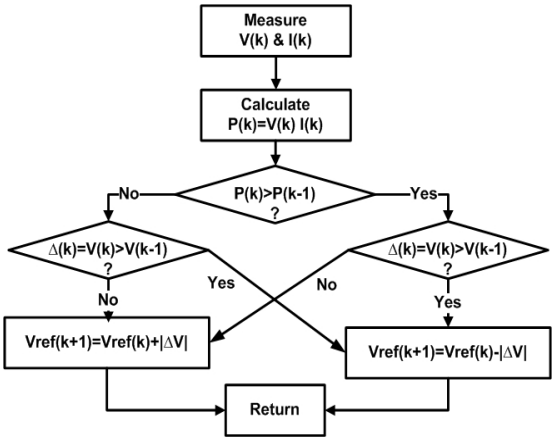

Fig. 2 P&O MPPT algorithm

D. Voltage Source Inverter

Fig. 3 shows a basic two-level three phase (2L-3P) VSI in which P and N are positive and negative terminals, respectively, and O is a null point. The VSI has three legs with two switches and two anti-parallel diodes on each. To prevent from short circuits across terminals, switches of the same leg should never be turned on simultaneously. Similarly, switches of the same leg should never be turned off simultaneously to avoid uncertain, floating output voltage. Terminals A, B, C can be connected to three phase load or to PEG, depending on off-grid or on-grid operation.

Conventionally, the output voltage is controlled by a

variation of Pulse Width Modulation (PWM) scheme, where pulse width is adjusted by increasing or decreasing on and off times of switches to control the output voltage. On and off commands are issued by comparing three phase modulating signals (V_{mA}, V_{mB}, V_{mC}) with a carrier wave (V_c), given by (6):

$$V_{xN} = \begin{cases} V_{DC} \; if \; V_{mx} > V_c \\ 0 \quad if \; V_{mx} < V_c \end{cases} \tag{6}$$

where x=A,B,C

If $V_{mX}>V_X$, $V_{XN}=V_{DC}$ with S_1 on, and S_4 off. On the other hand, if $V_{mX}<V_X$, $V_{XN}=0$ with S_1 off, and S_4 on. The status of switches for all three legs is shown in Table I.

A voltage source inverter can assume only 8 distinct switching states (Table II) since the input lines are never shorted and the output current is always kept continuous.

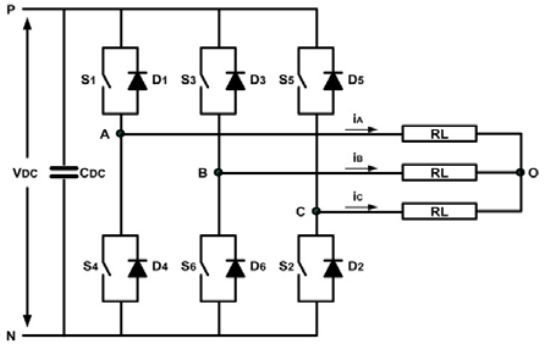

Fig. 3 2L-3P VSI

Individual phase voltages on the load can easily be determined considering the fact that any switching combination will result in a specific configuration of the VSI circuit. Fig. 4 shows VSI circuit configuration when $S_1S_2S_3$=111. Phases A and B are connected to the P terminal of V_{DC} while phase C is connected to the N terminal of V_{DC} (voltage across C_{DC}) and all 3 phases are connected to O point through load. This configuration puts load A and B in parallel, connected in series with load C and the DC source, which gives $V_{AO}=V_{BO}=1/3V_{DC}$ and $V_{CO}=-2/3V_{DC}$.

TABLE I
THE STATUS OF SWITCHES IN INDIVIDUAL LEGS

S States	Leg A			Leg B			Leg C		
	S_1	S_4	V_{AN}	S_3	S_6	V_{BN}	S_5	S_2	V_{CN}
P	1	0	V_{DC}	1	0	V_{DC}	1	0	V_{DC}
O	0	1	0	0	1	0	0	1	0

Line to line voltages, V_{AB}, V_{BC}, V_{CA}, are obtained by subtracting line to neutral voltage of one phase from the other. For example, V_{AB} is calculated by (7). Table III shows the phase load voltages and line to line voltages.

$$V_{AB} = V_{AN} - V_{BN} \tag{7}$$

TABLE II
VSI 8 SWITCHING STATES

Legs Upper S			Legs Lower S			Voltage		
S_1	S_3	S_5	S_4	S_6	S_2	V_{AN}	V_{BN}	V_{CN}
0	0	0	1	1	1	V_{DC}	V_{DC}	V_{DC}
0	0	1	1	1	0	V_{DC}	V_{DC}	0
0	1	0	1	0	1	V_{DC}	0	V_{DC}
0	1	1	1	0	0	V_{DC}	0	0
1	0	0	0	1	1	0	V_{DC}	V_{DC}
1	0	1	0	1	0	0	V_{DC}	0
1	1	0	0	0	1	0	0	V_{DC}
1	1	1	0	0	0	0	0	0

E. Control

Conventionally, VSI are controlled by one of the schemes discussed above, such as PWM and SVPWM. These schemes convert the three phase AC signal from a three phase reference frame to a two phase reference frame. These *αβ0* (dq0) are then regulated by PI controllers to export active power P and/or reactive power Q. The PWM controller simply compares the output of the regulators with triangular carrier wave to produce the required switching sequence. However, as indicated at the beginning, these techniques have issues such as poor performance of the PI controller with PEG harmonics, required switching dead time, PI controllers tuning based on a compromise between robustness and transient performance, carrier and modulating wave requirements, etc.

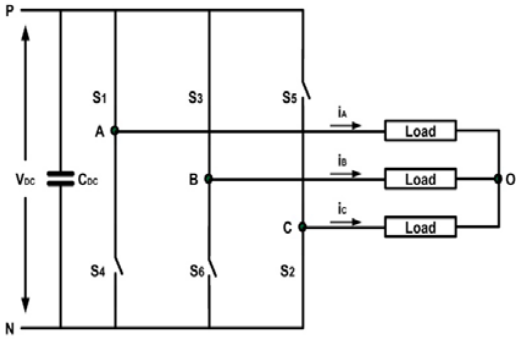

Fig. 4 VSI circuit for $S_1S_2S_3$=111

IV. MODEL PREDICTIVE CONTROL

Model predictive control strategies take advantage of the fact that only a finite number of possible switching states are associated with VSI. These states are discrete and the model of the system can be used in association with a discrete-time model of the load to predict the behavior of VSI system. The objective function, a selection criterion, is defined for choosing the optimum future variables corresponding to the optimal future switching state that minimizes the objective function, i.e., predict output currents that track the reference currents with minimal error. For each sampling period prediction, the output currents are measured and compared with the reference currents to minimize error. A smaller sampling period is selected to facilitate the assumption of a fixed reference current for that period.

TABLE III
PHASE LOAD AND LINE TO LINE VOLTAGES

Lower leg Sw			Phase load V*			Line-Line V*		
S_4	S_6	S_2	V_{AO}	V_{BO}	V_{CO}	V_{AB}	V_{BC}	V_{CA}
1	1	1	0	0	0	0	0	0
1	1	0	-1/3	-1/3	2/3	0	-1	1
1	0	1	-1/3	2/3	-1/3	-1	1	0
1	0	0	-2/3	1/3	1/3	-1	0	1
0	1	1	2/3	-1/3	-1/3	1	0	-1
0	1	0	1/3	-2/3	1/3	1	-1	0
0	0	1	1/3	1/3	-2/3	0	1	-1
0	0	0	0	0	0	0	0	0

* multiply all V's V_{DC}

MPC is exercised in $\alpha\beta$ reference frame with 6 active (non-zero voltage) and 2 zero (zero voltage) vectors. In addition, load dynamics are modeled as:

$$v = L\frac{di}{dt} + Ri \tag{8}$$

where R and L are load resistance and inductance, respectively, i is the load current and v is the VSI generated voltage vector.

Using Euler-Forward equation, the load current is approximated by:

$$\frac{di}{dt} \cong \frac{i(k+1)-i(k)}{T} \tag{9}$$

Using (8) and (9), we can say:

$$i^p\,(k+1) = \left(1 - \frac{RT}{L}\right) i(k) + \frac{T}{L} v(k) \tag{10}$$

where k=t (present) and k+1=t+1(future/predicted).

The predicted load current in (10) in the $\alpha\beta$ reference frame can be expressed as:

$$\begin{bmatrix} i_{\alpha(k+1)} \\ i_{\beta(k+1)} \end{bmatrix} = \begin{bmatrix} 1 - \frac{RT}{L} & 0 \\ 0 & 1 - \frac{RT}{L} \end{bmatrix} \begin{bmatrix} i_{\alpha(k)} \\ i_{\beta(k)} \end{bmatrix} + \begin{bmatrix} \frac{T}{L} & 0 \\ 0 & \frac{T}{L} \end{bmatrix} \begin{bmatrix} v_{\alpha(k)} \\ v_{\beta(k)} \end{bmatrix} \tag{11}$$

Equation (11) is used to predict the load current for each switching possibility. The objective function is evaluated for each of the eight possible voltage vectors generated by the VSI in order to calculate the future optimal value of the load current. The optimal value of objective function is applied during the next sampling period. Fig. 5 shows the VSI MPC control system.

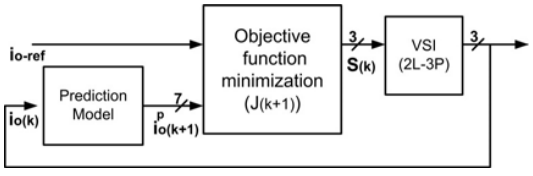

Fig. 5 VSI MPC control block diagram

TABLE IV
VSI SPACE VECTORS

S_4	S_6	S_2	Vector	V_x
1	1	1	0	V_0
1	1	0	$2/3V_{DC}$	V_1
1	0	1	$1/3V_{DC} + j\sqrt{3}/3V_{DC}$	V_2
1	0	0	$-1/3V_{DC} + j\sqrt{3}/3V_{DC}$	V_3
0	1	1	$-2/3V_{DC}$	V_4
0	1	0	$-1/3V_{DC} - j\sqrt{3}/3V_{DC}$	V_5
0	0	1	$1/3V_{DC} - j\sqrt{3}/3V_{DC}$	V_6
0	0	0	0	V_7

Fig. 6 outlines step by step implementation process of MPC for predictive control of VSI. First all the variables are initialized and values assigned (Data). This is followed by a process dynamic model of VSI based on the values for voltage vectors V_0 to V_7 (Table III). Then a set of control actions or manipulated variables $U_{(k)}$ based on operational principles (process experience) is developed corresponding to all possible output states (using switching states $S_4S_6S_2$ in Table IV). The current states of the system are measured ($i_{o\text{-}ref}$, $i_{o(k)}$) including switching states of $v_{(k)}$, and future outputs $Y_{(k+1)}$ (future currents $i_{o(k+1)}$) for k=1 to N are predicted using (11).

Objective function J (12) is used to minimize the error between the predicted output, $Y_{(k)}$, and the measured reference, $i_{o\text{-}ref}$ ($r_{(k)}$). The optimal $J_{(k+1)}$ with minimum error between the predicted and measured currents is selected and the corresponding control action, $U_{(k)}$, from the control action set, U = [000 001 010 011 100 101 110 111], is applied across VSI in the next sampling period. The output is observed and the process is repeated. Note that in each sampling period 8 predictions are made and 8 Js are evaluated before selecting the control action, $U_{(k)}$, for the next sampling period.

$$\min J_{(k+1)} = \sum_{k=1}^{k+N-1} (Y_{(k)} - r_{(k)}) \tag{12}$$

V. SIMULATION RESULTS

To evaluate the effectiveness of the MPC model, a 30kW VSI model was connected to 35.7 kW PV array. The array was designed with 119 modules, 300W each, with 7 strings of 17 modules connected in series. The system was subjected to varying irradiance and/or temperature to verify the model in different operating conditions. The modelled VSI can take 1000V at input and produces 480V at output, while voltage at PCC is 600V. Therefore, a transformer is interfaced between VSI and PEG to match the voltage of PCC. System frequency is 60Hz.

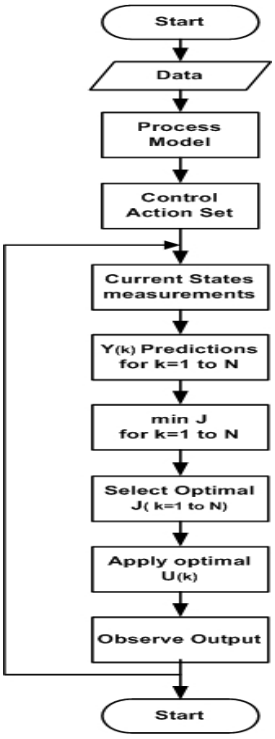

Fig. 6 MPC algorithm

Fig. 7 shows model subjected to varying irradiance (750, 900 and 600 W/m^2). Four different powers are reported, PV array DC power, VSI output AC power at 480V, Power at the utility side of the transformer at 600V, and power from utility at 600V to supply 50kW connected local load. Fig. 7 shows that VSI follows increments or decrements of power on the DC PV array side due to changes in the light condition (or changes in temperature, or both) with some loss (since Pac is less than Pdc) and grid supplies the remaining to the load. VSI output power added to the PEG supplied power gives us the load demand power at any instant. Also note that power at the output of transformer is less than the VSI output power due to transformer and other losses.

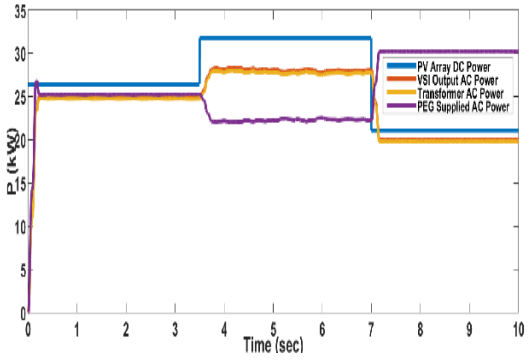

Fig. 7 Power Graphs

Fig. 8 shows VSI output parameters for phase A. Va and Vab are sinusoidal in nature and are at the expected levels of 277 and 480V. Phase A current is also sinusoidal and varies with changes in reference power due to changes in PV array DC power in response to increments or decrements in the solar irradiance. Pa successfully follows the changes and increase/decrease accordingly. Note that Pa is less than Pdc due to losses.

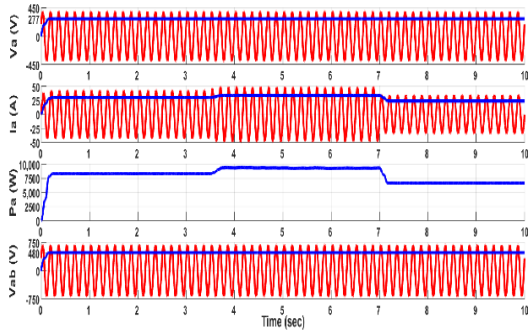

Fig. 8 VSI Output Parameters

Fig. 9 depicts the same parameters as in Fig. 8 but on the 600V side of the transformer. Again, signals are sinusoidal and successfully track the reference, as shown by changes in currents and power. As expected, the power is lower than Pa of VSI output due to losses.

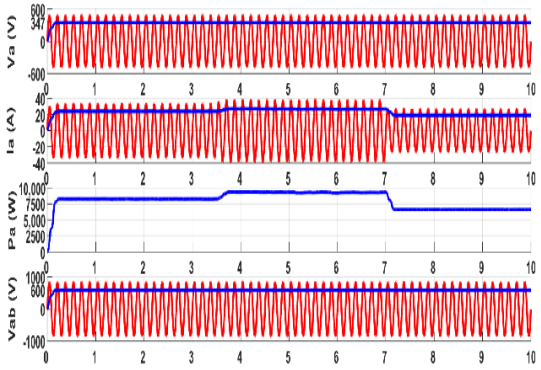

Fig. 9 V_s and i_s at varying P

This paper presented MPC of a UI-TPI for a PV system. The MPC based UI-TPI model resulted in a simpler control and implementation without sacrificing quality and accuracy. The poor performance and saturation of conventional PWM and PI regulators can be avoided by MPC. The adequacy of the MPC model in tracking the reference was validated in Matlab/Simulink.

ACKNOWLEDGMENT

The authors would like to thank Green Management Group, Inc. and Mitacs Inc. Canada for funding of this research project.

REFERENCES

[1] R. J. Wai, C. Y. Lin, Y. C. Huang, and Y. R. Chang, "Design of high-performance stand-alone and grid-connected inverter for distributed generation applications," IEEE Trans. Ind. Electron., vol. 60, no. 4, (2013).
[2] C. Trujillo, D. Velasco, G. Garcera, E. Figueres, and J. Guacaneme, "Reconfigurable control scheme for a PV micro-inverter working in both grid-connected and island modes," IEEE Trans. Ind. Electron., vol. 60, no. 4, (2013).
[3] M. Monfared, S. Golestan, and Josep M. Guerrero, "Analysis, Design, and Experimental Verification of a Synchronous Reference Frame Voltage Control for Single-Phase Inverters" IEEE Trans. Ind. Electron., vol. 61, no. 1, (2014).
[4] The world wind energy association "world wind energy report 2009" (http://www.wwindea.org/home/images/stories/worldwindenergyreport2009_s.pdf) (accessed February, 2014).
[5] The National Renewable Energy Lab report "2012 Renewable Energy Data Book" (http://www.nrel.gov/docs/fy14osti/60197.pdf) (accessed February, 2014).
[6] M. D. Singh, "Power Electronics," 2nd edition, Tata McGraw-Hill, 2007, ISBN:0-07-058389-7.
[7] M. H. Rashid, "Power Electronics Circuits, Devices, and Applications," 3rd edition, Pearson Prentice Hall, 2007, ISBN:81-317-0246-4.
[8] B. K. Boss, "Modern Power Electronics and AC Drives," Pearson Prentice Hall, 2007, ISBN:81-7758-876-1.
[9] G. Paul, S. A. Kannan, N. Johnson, and J. George, "Modeling And Analysis of PV Micro-Inverter", International Journal Of Innovative Research In Electrical, Electronics, Instrumentation and Control Engg., Vol. 2, Issue 2, (2014).
[10] I. M. Syed and K. Raahemifar, "Alternating Current Photovoltaic Module Model", Intl. J. of Elec., Comp., Electro., and Comm., Eng. Vol:9, No:3, (2015).
[11] M. Monfared, S. Golestan, and J. M. Guerrero, "Analysis, Design, and Experimental Verification of a Synchronous Reference Frame Voltage Control for Single-Phase Inverters" IEEE Trans. Ind. Electron., vol. 61, no. 1, (2014).
[12] I. M. Syed and K. Raahemifar, "Model Predictive Control of Single Phase Inverter for PV System", Intl. J. of Elec. Comp. Electro. and Comm. Eng., vol. 8, No:11, (2014).
[13] W. Oh, S. Han, S. Choi, and G. Moon, "Three Phase Three-Level PWM Switched Voltage Source Inverter With Zero Neutral Point Potential", IEEE Transactions on P. Electro., vol: 21, (2006).
[14] D. Yuan, G. Xu, B. Hu and A. Xiang, "Three Phase Three-Level PWM Switched Voltage Source Inverter with Zero Neutral Point Potential", IEEE Vehicle P. and Propulsion Conf., (2008).
[15] M. Rivera, J. Rodriguez, V. Yaramasu and B. Wu, "A Simple Current Control Strategy for Two-Level Four-Leg Inverters: The Model Predictive Approach", 4th Intl. Conf. on P. Eng., Energy and Elec. Drives, Istanbul, Turkey, (2013).
[16] I. M. Syed and K. Raahemifar, "Space Vector PWM and Model Predictive Control for Voltage Source Inverter Control", Intl. J. of Elec. Comp. Elctro. and Comm. Engg., vol. 8, (2014).
[17] K. Zhang, Y. Kang, J. Xiong, and J. Chen, "Direct repetitive control of SPWM inverter for UPS purpose," IEEE Trans. Power Electron., vol. 18, no. 3, (2003).
[18] P. Mattavelli, "An improved deadbeat control for UPS using disturbance observers," IEEE Trans. Ind. Elec., vol. 52, no. 1, (2005).
[19] T. L. Tai and J. S. Chen, "UPS inverter design using discrete-time sliding mode control scheme," IEEE Trans. Ind. Electron., vol. 49, no. 1, (2002).
[20] M. Mosa, H. Abu-Rub, M. E. Ahmed, A. Kouzoul, J. Rodríguez, "Control of Single Phase Grid Connected Multilevel Inverter Using Model Predictive Control", 4th International Conference on Power Engineering, Energy and Electrical Drives Istanbul, Turkey, (2013).
[21] J. Rodríguez, Pontt, C. Silva, P. Correa, P. Lezana, P. Cortés, U. Ammann, "Predictive current control of a voltage source inverter," IEEE Transactions on Industrial Electronics, vol. 54, no. 1, (2007).
[22] V. Yaramasu and B. Wu, "Predictive Control of a Three-Level Boost Converter and an NPC Inverter for High-Power PMSG-Based Medium Voltage Wind Energy Conversion Systems", IEEE Transactions on P. vol. 29, (2014).